Cauchy-Characteristic Matching: A New Approach to Radiation Boundary Conditions

Nigel T. Bishop,[1,2] Roberto Gomez,[2] Paulo R. Holvorcem,[3,5] Richard A. Matzner,[3]
Philippos Papadopoulos,[2,4] and Jeffrey Winicour[2]

[1]*Department of Mathematics, Applied Mathematics and Astronomy, University of South Africa, P.O. Box 392, Pretoria 0001, South Africa*

[2]*Department of Physics and Astronomy, University of Pittsburgh, Pittsburgh, Pennsylvania 15260*

[3]*Center for Relativity, University of Texas at Austin, Austin, Texas 78712-1081*

[4]*Department of Astronomy & Astrophysics, The Pennsylvania State University, University Park, Pennsylvania 16802*

[5]*Departamento de Matemática, Instituto de Matemática, Estatística e Ciência da Computação, Universidade Estadual de Campinas, Campinas, SP 13081-970, Brazil*

(Received 2 February 1996)

We investigate a new methodology for computing wave generation, using Cauchy evolution in a bounded interior region and characteristic evolution in the exterior. Matching the two schemes eliminates usual difficulties such as backreflection from the outer computational boundary. Mapping radiative infinity into a finite grid domain allows a global solution. The matching interface can be close to the sources, the wave fronts can have arbitrary geometry, and strong nonlinearity can be present. The matching algorithm dramatically outperforms traditional radiation boundary conditions. [S0031-9007(96)00365-1]

PACS numbers: 04.25.Dm, 04.30.Db

We present a new computational approach to radiation boundary conditions, based on discretizing an exact treatment of the radiation from source to infinity. The numerical solution therefore converges to the exact analytic solution of the radiating system, as we show. This is in contrast to usual radiation boundary conditions [1–4], which involve an approximation that does not converge to the exact solution. *Our algorithm converges to second order so that any desired accuracy can be achieved by refining the grid; no amount of grid refinement can lower the error of the traditional approach beyond a certain level.* This is manifest even at moderate resolutions, where our method has an error 2 orders of magnitude below that of traditional schemes. Here we treat scalar waves but the method is being used in the binary black hole grand challenge to calculate gravitational radiation. It has applicability to a wide range of hyperbolic systems, e.g., acoustic wave generation in nonlinear hydrodynamics and light emission in a nonlinear medium.

Traditional Cauchy methods impose artificial conditions at the computational boundary [1–4], typified by the well known Sommerfeld outgoing radiation condition which is strictly valid only at an infinite distance from the sources. This introduces an error of analytic origin, which persists even in high resolution simulations. Improvement by moving the boundary to a larger radius is computationally very expensive in three-dimensional simulations. An exact treatment of the boundary is possible if the retarded Green's function is known [5] but in a nonlinear problem this approach can be carried out only by a perturbation approximation.

In contrast, a characteristic formulation [6] can be compactified [7], mapping radiative infinity (the asymptotic limit of ougoing characteristics) to a finite coordinate radius. This provides a finite grid boundary, with no loss of accuracy because of the very simple asymptotic behavior of outgoing waves along characteristics. Only in a characteristic approach is there no need of an artificial outer boundary condition, because we can discretize the whole physical domain, with the outer boundary where the true radiation zone wave form can be identified.

A global characteristic approach must deal with caustics where the characteristics focus [8]. In hydrodynamics or general relativity, the caustic structure is dynamic and would have to be computed along with the evolution. These problems make it difficult to use the characteristic formulation in the near-field region but it proves to be both accurate and computationally efficient in the treatment of an exterior, caustic-free region [9].

Our procedure is a matched Cauchy-characteristic evolution [10–14]. A *Cauchy* formulation evolves a 3-space of field values step by step forward in time t; a *characteristic* formulation [6,9] evolves three-dimensional characteristic "cones" forward in *retarded* time u; see Fig. 1. The characteristic algorithm then provides an *outer* boundary condition for the interior Cauchy evolution, with infinity rigorously included in a compactified grid. The Cauchy algorithm supplies the *inner* boundary condition for the characteristic evolution. For nonlinear systems, such Cauchy-characteristic matching is much more computationally efficient than alternative methods of obtaining highly accurate wave forms [15]. Our work is the first systematic study of the stability and accuracy of this method.

Consider the scalar wave equation for $\phi(x, y, z, t)$,

$$\partial_{tt}\phi = \nabla^2\phi + F(\phi) + S(x, y, z, t), \qquad (1)$$

with nonlinear self-coupling $F(\phi)$ and external source S.

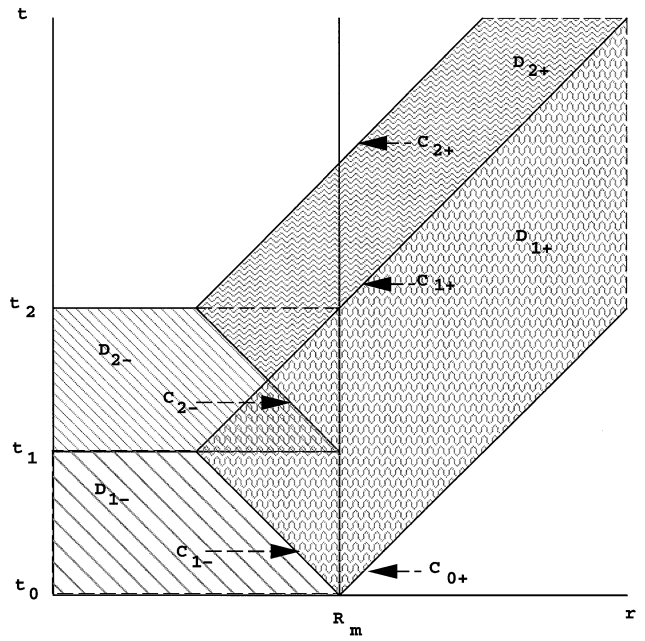

FIG. 1. Initial Cauchy data are evolved from t_0 to time t_1 throughout the region D_{1-}. Characteristic data induced on C_{1-}, combined with the initial characteristic data on C_{0+}, are used to evolve the region D_{1+}. This produces Cauchy data at time t_1 in the region $r \leq R_m$. Similarly, Cauchy evolution is used in the region D_{2-}, bounded on the right by C_{2-}. The characteristic data induced on C_{2^-}, together with those on C_{1+}, are sufficient to evolve through the region D_{2+}. The process can be iterated to obtain the entire future evolution.

In principle, $F(\phi)$ need only derive from a stable potential but for our approach to be computationally efficient ϕ must fall off as $1/r$ along the outgoing characteristics [9]. This rules out fields with nonzero rest mass, $F \sim \phi$, which decay exponentially along the characteristics. In a characteristic formulation (1) is expressed in standard spherical coordinates (r, θ, φ) and retarded time $u = t - r$:

$$2\partial_{ur} g = \partial_{rr} g - \frac{L^2 g}{r^2} + r(F + S), \qquad (2)$$

where $g = r\phi$ and L^2 is the angular momentum operator. The initial data are now $g(r, \theta, \varphi, u_0)$, on an initial outgoing characteristic cone $u = u_0$. [Since (2) is first order in u, $\partial_u g$ is not part of the initial data.]

In our matching scheme, the boundary $r = R_m$ of the interior domain may typically be placed just outside the radiating sources, and not necessarily many wavelengths away as in traditional approaches. We solve the interior Cauchy problem for (1) by standard second-order finite differencing on a Cartesian grid. We solve (2) in the exterior using a compactified radial coordinate $\xi(r)$, such that $\xi \sim C + D/r$ as $r \to \infty$, and a uniform grid $\xi_0, \xi_1, \ldots, \xi_M$ extending from $\xi = \xi(R_m)$ to $\xi = C$. The basic radial step along a characteristic cone is obtained by discretizing the identity which results from integrating (2) over a parallelogram bounded by ingoing and outgoing characteristics [9]. This numerical scheme is second-order accurate, and incorporates nonlinear and source terms in a consistent way. Rather than using spherical harmonics, we introduce a discretized representation of the angular momentum operator on the sphere, so that the term $L^2 g$ in (2) couples the various radial integrations.

The essential features of matching can be illustrated in spherical symmetry ($L^2 g = 0$). Let $G(r, t) = g(r, t - r)$. Consider initial Cauchy data $G(r, t_0)$ and $\partial_t G(r, t_0)$ in the region $0 \leq r \leq R_m$. These data determine a unique solution in the domain of dependence D_{1-}, whose outer boundary is the ingoing radial characteristic C_{1-} described by $t + r = t_0 + R_m$ (see Fig. 1). Although the source S is known for all times in the region $r \leq R_m$, the complete solution in the interior region $r \leq R_m$ requires additional information. In the case that no ingoing waves cross $r = R_m$, this information is that g vanish on the outgoing characteristic C_{0+} described by $u = t - r = t_0 - R_m$ (Fig. 1), i.e.,

$$g(r, t_0 - R_m) = 0, \qquad r \geq R_m . \qquad (3)$$

A unique solution of (1) over the exterior domain D_{1+} is determined by characteristic initial data consisting of (3) on C_{0+} and of the value of g on the characteristic C_{1-}. (The choice of physically appropriate initial data for general nonlinear problems is difficult and beyond the scope of the present work.)

The matching scheme proceeds as shown in Fig. 1. First, initial Cauchy data are evolved from t_0 to t_1 throughout the region D_{1-}, which is in its domain of dependence. D_{1-} is bounded on the right by the incoming characteristic segment C_{1-}. Next, the characteristic data induced on C_{1-} are combined with the initial characteristic data on C_{0+} to carry out a characteristic evolution throughout the region D_{1+}, bounded from the future by the characteristic C_{1+}. The solution determined from this initial stage induces Cauchy data at time t_1 in the region $r \leq R_m$, inside the matching boundary. This process can then be iterated to carry out the entire future evolution of the system.

Our matching algorithms are based upon a discretized version of this scheme in which the crisscross pattern of characteristics inside the radius R_m is at the scale of a grid spacing. Here we discuss two implementations from several possibilities which we have investigated.

In algorithm I, the boundary values for both the interior and exterior evolutions (i.e., the values of the field near $r = R_m$) are updated through one-dimensional cubic interpolations at constant time t, using previously computed field values from both the Cauchy and the characteristic grids. In a spherically symmetric code, this interpolation is naturally carried out along the radial direction, with two data points on the interior region and two data points in the exterior region. In three dimensions, we carry out the cubic interpolations along the Cartesian direction which is closest to the local radial direction at each boundary point.

In the second implementation, the continuity of the field and its normal derivative at $r = R_m$ are imposed more explicitly. At each time step, the boundary values for the characteristic evolution are supplied by interpolation on the interior grid; this ensures the continuity of the field in the continuum limit. The boundary values for the Cauchy evolution scheme are computed using a discrete version of the continuity condition for certain derivatives of the scalar field. In spherical symmetry, we impose the continuity of the radial derivative at constant retarded time u, which yields the condition

$$(\partial_t + \partial_r)G(r,t) = \partial_r g(r,u). \quad (4)$$

Neglecting the right-hand side of (4) yields the standard Sommerfeld condition, so we refer to the continuity condition (4) as a *generalized Sommerfeld condition*. The left-hand side of (4) is discretized using backward finite differences on the interior grid (as is usually done with artificial radiation conditions), and the right-hand side is evaluated by finite differencing on the exterior grid. It is also possible to impose the continuity of the second derivative, which yields a second-order generalized Sommerfeld condition. In three dimensions, we impose the continuity of the derivatives along the Cartesian direction which is closest to the local radial direction (at constant u). We denote the first- and second-order generalized Sommerfeld matching algorithms by C_1 and C_2, respectively. We will compare their performance to the Sommerfeld-like conditions S_1 and S_2 which are obtained by neglecting the right-hand sides of the generalized Sommerfeld conditions used in algorithms C_1 and C_2.

We carried out numerical experiments on the following aspects of the Cauchy-characteristic algorithms.

(a) Stability.—Long-term integrations of high frequency initial data indicate substantial regions of stability in the space of grid parameters $\rho = \Delta t/h$, $\alpha = h_{\rm ang}/h$, and $\beta = h_{\rm rad}/h$, where Δt is the time step, h is the Cauchy grid spacing, and $h_{\rm ang}$, $h_{\rm rad}$ are, respectively, the angular and radial grid spacings of the exterior grid at $r = R_m$. Algorithms C_i were generally stable for $\alpha > 1$, $\beta = O(1)$, and $\rho < \rho_{\rm CFL}$, where the bound $\rho_{\rm CFL}$ is imposed by the Courant-Friedrichs-Lewy condition for the interior and exterior evolution algorithms. Algorithm I was stable for $\alpha < 1.2$, $\beta = O(1)$, and $\rho < \frac{1}{2}\rho_{\rm CFL}$. Stability is robust with respect to reasonable changes in the parameters which were held fixed in the stability study.

(b) Convergence.—The experiments involve linear and nonlinear situations with grids of several resolutions. The Richardson extrapolation technique was used to accelerate the convergence of the numerical solutions.

(c) Comparison with traditional radiation conditions.—The matching schemes were compared to pure Cauchy schemes using the Sommerfeld-like conditions S_1 and S_2.

(d) Sensitivity of the numerical solutions to the position of the matching interface.—For each fixed value of R_m, a matched numerical solution should converge to the exact solution of the global initial-value problem. In general, a solution obtained using artificial radiation conditions converges to a limit which depends on R_m. (This limit should approach the exact solution when $R_m \to \infty$.)

The performance of our algorithms is summarized in Figs. 2 and 3 which show the error for a matching code [Fig. 2(b)], 2 orders of magnitude better than the performance of a Sommerfeld-like condition [Fig. 2(a)];

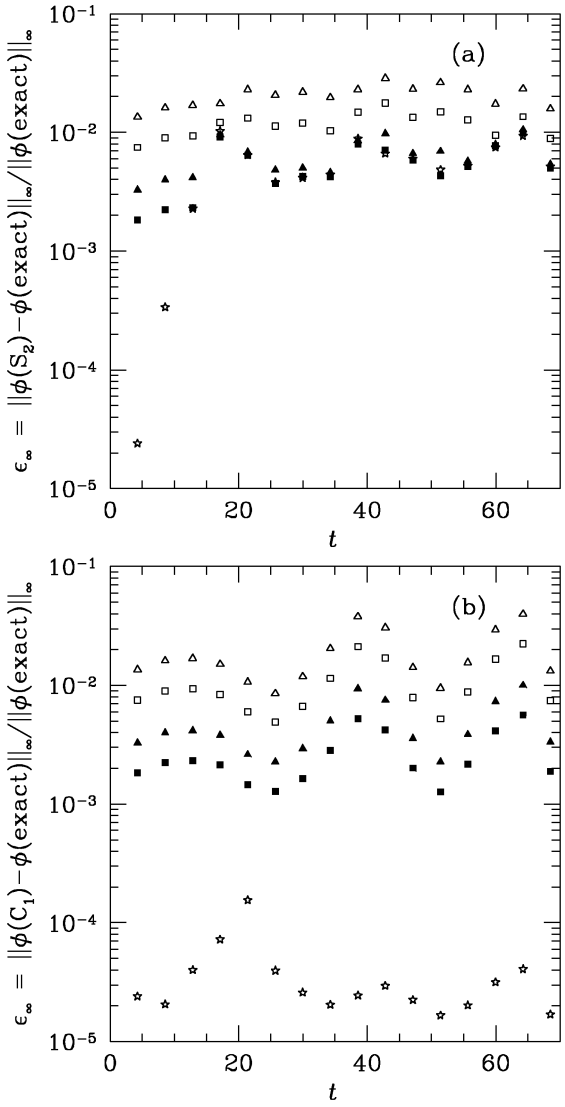

FIG. 2. Comparison between two algorithms for solving a forced linear wave equation: S_2 (a) and C_1 (b). The system consists of four nonspherical sources positioned nonsymmetrically in the interior. Relative errors over the interior grid are shown for selected times using four progressively finer discretizations in the proportion 8 (open triangles) : 6 (open squares) : 4 (solid triangles) : 3 (solid squares). The errors resulting from applying Richardson extrapolation to the results for the finest grids are indicated by stars. It can be seen that the matching solution (b) is about 2 orders of magnitude more accurate than the solution using the Sommerfeld-like condition (a).

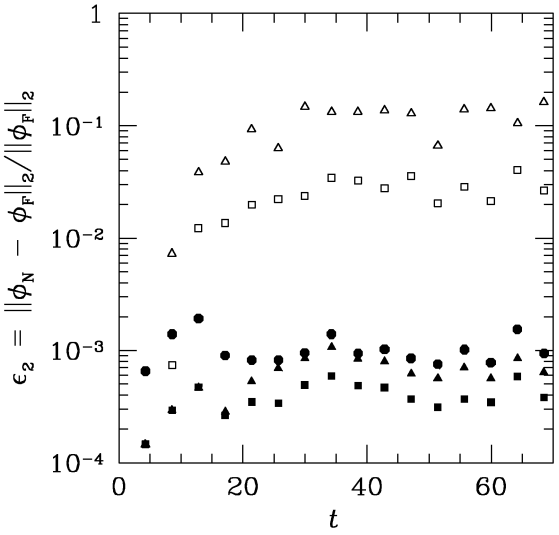

FIG. 3. Sensitivity of the numerical solutions of the strongly nonlinear forced wave equation $\partial_{tt}\phi = \nabla^2\phi - 4\phi^3 + S$ to changes in R_m. The source has support on two ellipsoids positioned nonsymmetrically in the interior. The data in the figure correspond to algorithms S_1 (open triangles), S_2 (open squares), C_1 (solid triangles), C_2 (solid squares), and I (solid circles). For each algorithm, we show the difference between the Richardson-extrapolated interior solutions obtained for $R_m = 182/17$ and $R_m = 234/17$, as measured by the ratio ϵ_2 defined in the text. Note the substantial insensitivity of the three matching algorithms (solid symbols).

and which show the expected insensitivity of the matching algorithms to the position of the Cauchy-characteristic interface (Fig. 3), again about 2 orders of magnitude better than Sommerfeld-like conditions S_1 and S_2.

We estimate the accuracy of the algorithms by comparing numerical solutions at different resolutions, and their Richardson extrapolates, to an exact solution. Figure 2 displays the numerical error in the Cauchy region for a nonspherical forced linear problem (with known solution). The error obtained with the Sommerfeld-like condition S_2 [Fig. 2(a)], initially decreases with grid spacing, but approaches a limiting value of about 0.6% in the l_∞ norm, $||\phi||_\infty = \max_{\text{grid}}|\phi|$. ($S_1$ exhibits similar behavior, but with a limit of about 2.0%.) In contrast, the error for matching algorithms such as C_1 steadily decreases with resolution [Fig. 2(b)]; a dramatic reduction in error is obtained by second-order Richardson extrapolation [star symbols in Fig. 2(b)], with error as small as 0.002% in the l_∞ norm. These results confirm the expected second-order convergence of the matching algorithms.

Figure 3 compares matching and Sommerfeld-like algorithms in a strongly nonlinear, nonspherical problem. For arbitrarily fine discretizations, increasing the radius R_m of the Cauchy region by the factor 1.29 affects the solutions using S_1 and S_2 by 15% and 3%, respectively (as measured by $\epsilon_2 \equiv ||\phi_N - \phi_F||_2/||\phi_F||_2$, where ϕ_N and ϕ_F are the numerical solutions corresponding to R_m and $1.29R_m$, and $||\phi||_2 \equiv \langle\phi^2\rangle^{1/2}$ averaged over grid points inside $0.93R_m$). As expected, all three matching codes are essentially insensitive to R_m. (The Richardson extrapolates for different R_m typically differ by only 0.06%.) Furthermore, numerical experimentation indicates that even this small sensitivity decreases with finer discretizations. This is strong evidence that the matching codes converge to the true solution of the nonlinear problem. Further details will be reported elsewhere [16].

This work was supported by the Binary Black Hole Grand Challenge Alliance, NSF PHY/ASC 9318152 (ARPA supplemented), by NSF PHY 9310083, by a Cray Research grant to R. A. M., and by NSF PHY 9510895 to the University of Pittsburgh. N. T. B. thanks the South African FRD for financial support and the University of Pittsburgh for hospitality during a sabbatical. P. R. H. was supported by Fundação de Amparo à Pesquisa do Estado de São Paulo, Brazil under Grant No. 93/5008-4. Computer time was provided by the Pittsburgh Supercomputing Center under Grants MCA94P015P to R. A. M. and PHY860023P to J. W. and by the Center for High Performance Computing Facility of the University of Texas at Austin.

[1] E. Lindman, J. Comput. Phys. **18**, 66 (1975).
[2] M. Israeli and S. A. Orszag, J. Comput. Phys. **41**, 115 (1981).
[3] R. Higdon, Math. Comp. **47**, 437 (1986).
[4] R. Renaut, J. Comput. Phys. **102**, 236 (1992).
[5] J. De Moerloose and D. De Zutter, IEEE Trans. Antennas Propag. **41**, 890 (1993).
[6] F. G. Friedlander, *The Wave Equation on a Curved Space-Time* (Cambridge Univ Press, Cambridge, 1975), Chap. 5, p. 193.
[7] R. Penrose, Phys. Rev. Lett. **10**, 66 (1963).
[8] H. Friedrich and J. M. Stewart, Proc. R. Soc. London A **385**, 345 (1983).
[9] R. Gómez, J. Winicour, and R. Isaacson, J. Comput. Phys. **98**, 11 (1992).
[10] N. Bishop, in *Approaches to Numerical Relativity*, edited by R. d'Inverno (Cambridge Univ. Press, Cambridge, 1992).
[11] N. Bishop, Classical Quantum Gravity **10**, 333 (1993).
[12] C. Clarke and R. d'Inverno, Classical Quantum Gravity **11**, 1463 (1994).
[13] C. Clarke, R. d'Inverno, and J. Vickers, Phys. Rev. D **52**, 6863 (1995).
[14] M. Dubal, R. d'Inverno, and C. Clarke, Phys. Rev. D **52**, 6868 (1995).
[15] N. Bishop, in *3rd Texas Workshop on 3-Dimensional Numerical Relativity*, edited by R. Matzner (U. of Texas, Austin, 1996).
[16] N. Bishop *et al.* (to be published).